

A probabilistic Bayesian methodology for the strain-rate correction of dynamic CPTu data

Stefano Collico^{1*}, Marcos Arroyo¹, Achim Kopf², Marcelo Devincenzi³

¹Department of Environmental and Civil Engineering (DECA), Universidad Politècnica de Catalunya (UPC), Barcelona, Spain.

²Center for Marine Environmental Science (MARUM), Bremen, Germany.

³ Geociencias y Exploraciones Marítimas, Sant Cugat del Vallès, Barcelona, Spain.

*Corresponding author: Stefano Collico; email: stefano.collico@upc.edu

Abstract

Dynamic Cone Penetration Tests (CPTu) profile offshore sediments by impact penetration. To exploit their results in full the measured data is converted to obtain a quasi-static equivalent profile. Dynamic CPTu conversion requires calibrated correction models. Calibration is currently done by using paired (i.e., very close) quasi-static and dynamic tests. It is shown here that paired test data, which may be inconvenient to acquire offshore, are not strictly necessary to convert dynamic CPTu data. A new probabilistic methodology is proposed to call upon quasi-static results from a much wider area in the conversion procedure. Those results feed the prior distribution of a converted profile, within a Bayesian updating scheme where strain rate coefficient and correction model error are also described by updated stochastic variables. The updating scheme is solved numerically using the Transitional Markov Chain MonteCarlo sampling algorithm. To avoid undue influence of local profile heterogeneity, the statistic treatment of the quasi-static CPTu data takes place in the frequency domain, using a discrete cosine transform (DCT). The new procedure is applied to a CPTu campaign offshore Nice (France): dynamic tests are converted with equal precision using quasi-static data acquired at distances orders of magnitude larger than what was previously employed.

Keywords: Dynamic CPTu, strain-rate coefficient, Transitional Markov Chain MonteCarlo, cone tip resistance, Nice.

1 Introduction

Free-fall penetrometers are increasingly used for offshore sediment characterization because of their rapid deployment capabilities and relative ease of operation (Randolph et al. 2018). Free-fall penetrometers with standard CPTu measurement capabilities (i.e., acquisition of tip resistance, sleeve friction and pore pressure) are particularly attractive, as they may potentially benefit from all the empirical and theoretical knowledge that underpins quasi-static CPTu data interpretation.

However, to achieve that potential, important obstacles need first to be surmounted. Dynamic CPTu is very different from quasi-static CPTu, as the soil is not tested at a constant penetration rate of 2 cm/s but instead at a variable velocity, starting at impact at several m/s. As a result, dynamic-CPTu records differ strongly from those of quasi-static CPTu, and they need to be corrected before being interpreted with the same tools as quasi-static tests (e.g., by using calibrated cone factors for undrained shear strength inference).

Different velocity-dependent mechanisms are present. The ability of pore water to flow around the instrument during its advance is affected by penetration speed. Penetration speed also changes the strain rate applied to the soil skeleton and, as is well known (Augustesen et al. 2004), most soils show some rate dependency. In very soft soils inertial drag effects around the penetrating object may also play a significant role. Several correction models (Lehane et al. 2009; Steiner et al. 2014; Chow et al. 2017) have been thus developed, incorporating one or more of these mechanisms.

However, even the most elaborated models currently available leave some basic observations unexplained, such as the differences between required tip and shaft resistance corrections. Moreover, all the proposed correction models require a number of empirical factors to be calibrated for specific soil conditions. Given those limitations, there are pragmatic reasons to favor relatively simple dynamic CPTu correction models. For fine grained soils, where even quasi-static CPTu are undrained and drainage effects are not an issue, those simpler models take the form of strain-rate CPTu corrections (Stoll et al. 2007; Buhler and Audibert 2012; Steiner et al. 2014).

Strain rate CPTu corrections are formulations where the effect of velocity on cone readings is embedded in a strain-rate coefficient *SRC*. For a given formulation the *SRC* is a function of the piezocone parameter (q_t , f_s , u_2) that is being converted, of soil type and piezocone geometry. The formulation of strain rate CPTu corrections was inspired by rate-effects observed on soil laboratory test or in other field tests, like the vane test (e.g., Biscontin and Pestana 2001). It is however recognized (Steiner et al. 2014) that, even if the corrections maintain the same form, the *SRCs* obtained elsewhere may not be directly applicable to the CPTu case and specific calibration is needed.

SRC calibration is then typically based on the comparison of static and dynamic CPTu records acquired in similar conditions. Similar conditions are easier to establish when testing in the laboratory (Dayal and Allen 1975; Chow et al. 2017) than when testing offshore. Ideally, the *SRC* would be estimated from paired (i.e., closely located in space and time) dynamic and quasi-static CPTu observations, (Steiner et al. 2014). In some circumstances, however, paired quasi-static readings may not be available and *SRC* values will have to be derived from literature, using the lithology deduced from nearby cores as a guide. Such procedure results in inherently unprecise *SRC* estimates, leading to underestimation or overestimation of the quasi-static equivalent profile, and therefore to increased geotechnical parameter uncertainty.

This study addresses that problem applying a probabilistic methodology to improve accuracy of *SRC* estimates when paired quasi-static CPTu profiles are unavailable. Conversion of dynamic

CPTu measurements using *SRC* is conceptualized as a transformation procedure involving some error, and the probabilistic distribution of that error is evaluated alongside that of the *SRC* coefficient. Evaluation of the relevant probability distributions is cast as a Bayesian updating problem, solved numerically using the Transitional Markov-Chain MonteCarlo algorithm (TMCMC), (Ching and Chen 2007; Ching and Wang 2016).

In the method proposed the probabilistic evaluation of *SRC* is computed simultaneously to the conversion of the dynamic record into a quasi-static equivalent profile. Prior knowledge relevant to the unknown quasi-static profile is obtained from quasi-static CPTu measurements previously acquired in the same offshore area –although at significant distances, i.e., unpaired with the dynamic CPTu that is being transformed. Manipulation and treatment of that information takes place in the frequency domain, using a discrete cosine transform function (i.e., DCT) (Candès et al. 2006; Zhao et al. 2018; Zhao et al. 2020). This avoids the problems of local spatial biases that might be caused by the sharp irregularities that -due to local heterogeneity- are pervasive in CPTu traces.

Although the methodology proposed has more general application, we focus on the correction of cone tip measurements. The method is illustrated by application to a set of dynamic CPTu data acquired nearshore Nice airport (France), an area well documented from previous studies (Dan et al. 2007; Steiner et al. 2015; Sultan et al. 2010).

2 Strain rate corrections for CPTu tip resistance

2.1 Strain rate correction models for homogenous fine-grained sediments

Strain rate effects on cone tip resistance are best formulated using normalized shear strain rates, which can be approximated by the ratio of cone velocity to cone diameter (Chung et al. 2006; Lehane et al. 2009). Therefore, a general formulation for a strain-rate correction will take the form

$$(1) \quad \frac{q_{t-dyn}}{q_{t-ref}} = F \left(\frac{\left(\frac{v_{dyn}}{d_{dyn}} \right)}{\left(\frac{v_{ref}}{d_{ref}} \right)} \right)$$

Where q_{t-dyn} represents dynamic cone tip resistance values, acquired with a cone of diameter d_{dyn} advancing at a velocity v_{dyn} , whereas q_{t-ref} represents a reference cone tip resistance, acquired with a cone of diameter d_{ref} advancing at a velocity v_{ref} .

The reference cone tip resistance q_{t-ref} is chosen so that it corresponds to a minimum in tip resistance, which roughly corresponds to the minimal penetration velocity resulting already on undrained conditions (Lehane et al. 2009; Chow et al. 2017). These nominally undrained conditions may be assessed through nondimensional velocity $V_{ref} = \frac{v_{ref} d_{ref}}{c_h}$, with c_h horizontal consolidation coefficient (Randolph and Hope 2004). Guidelines on V_{ref} values are reported by DeJong et al. (2013) and Steiner et al. (2014). For fine-grained sediments standard quasi-static CPTu result in undrained conditions when ($V_{ref} > 30$).

Three different strain-rate law formulations have been used for correcting CPTu tip records (Steiner et al. 2014). The logarithmic formulation is given by:

$$(2) \quad \frac{q_{t-dyn}}{q_{t-ref}} = 1 + SRC_{log-qt} \cdot \log \left(\frac{v_{dyn}}{d_{dyn}} / \frac{v_{ref}}{d_{ref}} \right)$$

with SRC_{log-qt} strain-rate coefficient of cone tip resistance.

An alternative formulation uses an inverse hyperbolic sine:

$$(3) \quad \frac{q_{dyn}}{q_{ref}} = 1 + SRC_{asinh-qt} \cdot asinh \left(\frac{v_{dyn}}{d_{dyn}} / \frac{v_{ref}}{d_{ref}} \right)$$

where $SRC_{asinh-qt} = SRC_{log-qt} / \ln(10)$.

A third formulation employs a power law:

$$(4) \quad \frac{q_{dyn}}{q_{ref}} = \left(\frac{v_{dyn}}{d_{dyn}} / \frac{v_{ref}}{d_{ref}} \right)^{SRC_{exp-qt}}$$

The logarithmic formulation is the one with longest tradition (e.g., Dayal et al. 1975; Aubeny and Shi 2006; Stoll et al. 2007; Steiner et al. 2012; Stephan et al. 2015). The inverse sine hyperbolic formulation avoids anomalous SRC values at very low velocities, when the probe is coming to rest. The power law function seems to capture rate effects better over larger ranges in strain rate (Biscontin and Pestana 2001). Typical SRC values for different strain-rate laws (i.e., average, lower and upper bound), for fine grained sediments were summarized by Steiner et al. (2014) and are reported in [Table 1](#).

2.2 Effect of coarse inclusions

The evaluation of strain-rate effects on penetration resistance is strongly influenced by sediment heterogeneity. Stoll et al. (2007) analyzed the effect of thin layers (i.e., thickness ≤ 10 cm) of dense sand included within fine-grained sediments on dynamic CPTu response.

Because the strain rate coefficient is soil type dependent, it should ideally be evaluated only where the dynamic CPTu record allows to consistently identify a particular soil layer (Stoll et al. 2007). However, subdivision of dynamic CPTu profiles is difficult, complicated by the nonlinear variation with depth of penetration velocity and strongly influenced by the analyst judgment and heuristics. In light of these considerations, a simplified approach is usually applied in practice, in which a single strain-rate coefficient is applied to the whole record (Steiner et al. 2014; Steiner et al. 2015).

2.3 Evaluation of the strain-rate coefficient, SRC

Using paired quasi-static CPTu observations Steiner et al. (2014) proposed to evaluate the fit achieved with SRCs using a Kolmogorov–Smirnov test (KS test; Steiner et al. 2012; Steiner et al. 2014). In the KS test the maximum error between cumulative density functions is evaluated. This error is expressed through a model fit coefficient denoted as R^2 :

$$(5) \quad R^2 = 1 - \max |F_1(\text{quasi-static}) - F_2(\text{converted dynamic})|$$

with $F_1(\text{quasi-static})$ cumulative density function of quasi-static CPTu measurements and $F_2(\text{dynamic})$ cumulative density function of corresponding dynamic CPTu measurements (Figure 1). The results of the KS test may be used to optimize the selection of SRCs for any given paired dynamic and quasi-static CPTu.

In absence of paired quasi-static CPTu readings, data conversion is performed using a range of SRC selected as a function of soil sample lithology (Table 1). There are several sources of error associated with this methodology. SRC from literature (Biscontin and Pestana 2001; Chung et al. 2006; Dayal and Allen 1975; Lehane et al. 2009; Stoll et al. 2007) are typically based on laboratory tests on homogenous soil samples covering only some soil types and properties. In-situ sediments to which they are applied may differ in terms of soil properties (e.g., water content, plasticity index PI , limit Liquid LL). Moreover, dynamic CPTu observations are affected by measurements error (e.g., inclination of rod during driving process, sediment heterogeneity), not present in laboratory SRC values. Given all those uncertainties it seems reasonable to address dynamic to static CPTu conversion within a probabilistic framework.

3 Probabilistic formulation of strain-rate correction

3.1 Bayesian formulation for the strain-rate correction

The proposed methodology aims to quantify the strain-rate coefficient and its uncertainty at a specific location by integrating information from all the quasi-static CPTu previously acquired in a relatively large zone around the dynamic CPTu test location. The evaluation of the *SRC* is made simultaneous with that of the transformed quasi-static profile, which is also expressed in a probabilistic manner. A Bayesian probabilistic framework is applied as it is ideally suited to incorporate pre-existing information on strain-rate coefficient and CPTu site-specific information.

From a Bayesian perspective, probability expresses a degree of belief on the outcome of an event or truth of a proposition, given some evidence (Vick 2002). Bayesian analysis is thus able to integrate, in a systematic and rational manner, existing prior information, sometimes subjective, with observed data. It is also easily adaptable to sequential procedures, incorporating the result of new observations as they become available. It is also able to integrate different type of uncertainties about specific problem inputs in a transparent and rational manner (Baecher and Christian 2005). It is therefore unsurprising that Bayesian analysis has become increasingly popular in geotechnical engineering, where varied uncertainty sources, staged information updates and the presence of existing, but sometimes vaguely specified, previous information are daily occurrences.

The Bayesian perspective on probability is conceptually different from the more traditional frequentist one. As succinctly explained by Contreras et al. (2018) frequentists treat statistical parameters (e.g., mean and standard deviation of error incurred by a geotechnical predictive model) as unknown fixed quantities, whereas the observations are treated as realizations of random variables. On the contrary, from a Bayesian perspective, parameters of statistical models are unknown random variables, and observations are fixed known quantities.

In the basic Bayesian inference scheme, some limited prior knowledge about the distributions of the problem random variables, Ω is updated considering the likelihood of the observations ξ , given the statistical model. This may be written (Gelman et al. 2013) as:

$$(6) \quad f''(\Omega|\xi) = n L(\Omega) f'(\Omega)$$

with n normalizing constant, $L(\Omega)$ denotes the likelihood, and $f''(\Omega)$ and $f'(\Omega)$ the posterior and prior distributions, respectively, of the problem random variables.

To apply the Bayesian scheme in our problem, we start by denoting $h(\boldsymbol{\theta})$ as the conversion model that relates static and dynamic cone tip resistance, using any of the strain rate correction models given by eq. (1-3). As an example, using the logarithmic strain-rate law of eq. (2):

$$(7) \quad h(\boldsymbol{\theta}) = \left[q_{t-static} \cdot \left(1 + SRC_{log-qt} \cdot \log \left(\frac{v_{dyn} d_{ref}}{v_{ref} d_{dyn}} \right) \right) \right]$$

$\boldsymbol{\theta}$ is a vector collecting the random variables explicit in the conversion model. The vector of unknown random variables $\boldsymbol{\theta}$ in this case includes the (unknown) static profile and the strain-rate coefficient, so that $\boldsymbol{\theta} = [(q_{t-static}), SRC_{log-qt}]$.

The model target, denoted by ξ , represents the dynamic CPTu observations (i.e., $\xi = q_{t-dynamic}$). The model output might differ from the target due to uncertainties beyond those explicit in the definition of $h(\boldsymbol{\theta})$. The difference between model output and measurements ξ is conceptualized as model error:

$$(8) \quad \xi = h(\boldsymbol{\theta}) + \varepsilon$$

The model error is described by a normal random variable with zero mean and unknown standard deviation σ_ε , $\varepsilon \sim N(0, \sigma_\varepsilon)$, meaning that $h(\boldsymbol{\theta})$ has no bias and is able to accurately reproduce the actual response of the system ξ within some precision σ_ε . A normal distribution for the model error ε is a common assumption in probabilistic assessment of geotechnical models (Zhang et al. 2009). We assume that the logarithmic SRC produces unbiased estimates based on previous performance (e.g., Steiner et al. 2015).

The standard deviation of model error is another random variable in our problem. Therefore, we have that $\boldsymbol{\Omega}$ vector of random variables (i.e., $\boldsymbol{\Omega} = [\sigma_\varepsilon, \boldsymbol{\theta}]$). The relevant likelihood for the observations in a dynamic CPTu record may be then formulated as the product of error probability for all the observations (Zhang et al. 2009):

$$(9) \quad L(\boldsymbol{\Omega}) = \prod_{i=1}^N \phi \left(\frac{\xi_i - h(\boldsymbol{\theta})}{\sigma_\varepsilon} \right)$$

with ϕ standard normal distribution and N number of data in the dynamic CPTu record. A general flowchart for the methodology applied is given in (Figure 2).

3.2 Representing the quasi-static CPTu profile in the probabilistic model

In the probabilistic model that we have presented each $q_{t-static_i}$ value of the (unknown) paired quasi-static CPTu profile that results from the strain-rate correction is conceptualized as a random variable. For the Bayesian inference scheme (eq. 6) we will have to propose a prior distribution of possible $q_{t-static_i}$ values. This will be done, as discussed below, with help from a database of “proximal” quasi-static CPTu data, collected within areas of several km². Now, CPTu data is highly sensitive to small spatial geological and stratigraphical variations, which are unlikely to have continuity at the scale of the “proximal” database and whose spatial variability will be very complex to be fully characterized within the model. If we assume that the “proximal” quasi-static data are independent and equally valid sources of information for the quasi-static prior, any small anomaly at a given depth in any CPTu record will have undue influence in the prediction, but only at that particular depth.

A way out of this problem is to express the “proximal” CPTu information that feeds the prior in the frequency domain, instead of the spatial domain. The presence of heterogeneities in the “proximal” database will thus affect the prediction, but not so their specific position within a particular record. To express CPTu profiles in the frequency domain we use a discrete cosine transform. This kind of frequency domain representation is robust -i.e., not overly affected by the eventual presence of local heterogeneities in the database- and easily scalable -i.e., able to deal with databases of different size.

The CPTu record is thus represented by a series of cosine components with different frequencies. The use of a DCT to represent and analyze CPTu records has several precedents, for instance (Zhao and Wang 2018; Zhao and Wang 2020) who use it to facilitate compressive sampling techniques (Candes et al. 2006). In this work, only the concept of discrete cosine transform function is applied and the application of compressive sampling is not considered.

Using a DCT any $q_{t-static}$ record on a depth interval z can be expressed as (Oppenheim and Schafer 1999):

$$(10a) \quad q_{t-static} = \sqrt{\frac{2}{N}} \sum_{n=1}^N q_{t-static}(u) \cos \left[\frac{\pi}{4N} (2n-1)(2u-1) \right]$$

with:

$$(10b) \quad q_{t-static}(u) = \sqrt{\frac{2}{N}} \sum_{n=1}^N q_{t-static} \cos \left[\frac{\pi}{4N} (2n-1)(2u-1) \right]$$

$u =$ frequency $u = 0, \dots, N-1$;

$N =$ total number of measurements that compose the $q_{t-static}$ profile.

As an example, [Figure 3b](#) reports the amplitude coefficients in frequency domain, (i.e., the $q_{t-static}(u)$) corresponding to the CPTu record ($q_{t-static}(z)$) reported in [Figure 3a](#).

Using the DCT representation the vector of unknown random variables $\theta = [q_{t-static}, SRC_{log-qt}]$ now contains the N transform coefficients. Substituting eq. (10a) into eq. (7) leads to:

$$(11) \quad h(\theta) = \left[\sqrt{\frac{2}{N}} \sum_{n=1}^N q_{t-static}(u) \cos \left[\frac{\pi}{4N} (2n-1)(2k-1) \right] \cdot \left(1 + SRC_{log-qt} \cdot \log \left(\frac{v_{dyn} d_{ref}}{v_{ref} d_{dyn}} \right) \right) \right]$$

with $\theta = [q_{t-static}(u), SRC]$ $N + 1$ unknown random variables.

3.3 Sampling algorithm

To evaluate the posterior density distribution $f''(\Omega|\xi)$ we use here the Transitional Markov-Chain MonteCarlo algorithm (TMCMC) proposed by Ching and Cheng (2007), as a generalization of the more widespread Metropolis-Hasting scheme. TMCMC has been used in many applications, including site geotechnical characterization based on CPTu (Ching et al. 2016) and constitutive model selection for rate dependent soils (Zhou et al. 2018).

Like other sampling algorithms (Bishop 2006) TMCMC obtains samples from the posterior distribution $f''(\Omega|\xi)$ so that it can be defined without integration, avoiding the computation of the normalizing constant n in the bayesian updating equation (eq. 6). TMCMC is particularly advantageous when the target posterior distribution is likely to have a complicated geometry, for instance because of having multiple modes, and/ or is difficult to visualize because the prior information is very uninformative.

The basic idea behind TMCMC algorithm is to iterate the bayesian updating scheme, using for the purpose a series of intermediate density functions constructed so as to finally converge to the posterior distribution $f''(\Omega|\xi)$ from the prior $f'(\Omega)$ (Ching and Chen 2007; Ching and Wang 2016):

$$(12) \quad f_j'(\boldsymbol{\Omega}) \propto f'(\boldsymbol{\Omega})L(\boldsymbol{\Omega})^{p_j} \text{ with } j = 0, \dots, J; \quad 0 = p_0 < p_1 < \dots < p_J = 1$$

with $j =$ stage number and $p_j =$ coefficients computed such that the transition from j to $j + 1$ stage is smooth. The p_j are selected to ensure a smooth transition between iterations. At $j = 0$ $f'(\boldsymbol{\Omega})$ in eq. (12) coincides with prior defined by $f_0'(\boldsymbol{\Omega})$, while for $j = J$ coincides with the joint posterior distribution $f_j'(\boldsymbol{\Omega}) = f''(\boldsymbol{\Omega}|\xi)$. A complete account of the TMCMC algorithm is given by Ching and Cheng (2007) and Ching et al. (2016).

The stochastic model analyzed here has some characteristics that made TMCMC attractive. To begin with $\boldsymbol{\Omega}$ is relatively high-dimensional, as it does include all the N coefficients in the DCT of the q_t -static. There is also the additional problem, derived from heterogeneity, of the possibility of multiple solutions, i.e., equally plausible combinations of generated static-CPTu profile and SRC coefficients. This means that the target density distribution $f''(\boldsymbol{\Omega}|\xi)$ might have a multimodal geometry (i.e., different peaks of high probability density). Collico (2022) verified that the performance of TMCMC in this problem was indeed superior to that of a simpler Metropolis-Hastings scheme.

3.4 Selection of prior knowledge

As stated above the correction model includes three stochastic variables: the vector of DCT coefficients for the quasi-static equivalent profile, the SRC and the standard deviation of model error. Prior distributions are required for all of them.

When selecting a prior for the quasi-static equivalent profile a preliminary question is to identify potentially relevant datasets from which the prior characteristics may be inferred. In other geotechnical applications of Bayesian inference, it is frequent to distinguish between “global” and “local” datasets, with “global” datasets being exploited to identify relevant priors. For instance, when elaborating a landslide susceptibility map, Collico et al. (2020) use a global dataset of clay properties to extract relevant priors for local geotechnical properties assigned to cells covering a very large area of the Atlantic Ocean. The stochastic variables being updated in that case represented material properties, such as normalized undrained strength. For that kind of variable, it is relatively easy to identify global datasets that may provide meaningful priors.

In this case the stochastic variable that is updated represents a quasi-static CPTu profile. A CPTu profile is an instrument response, reflecting material characteristics but also spatial arrangements (layering) and technological detail (as not all CPTu are the same, particularly offshore). Therefore, it is intrinsically more difficult to identify relevant “global” datasets from which priors can be

extracted. We have opted here to identify priors using a “proximal” dataset that is meaningful for the problem i.e., that of the quasi-static CPTu records available within the area of interest (identified by geological, geomorphological and geotechnical traits). In the example shown below that area corresponds to a continental margin section.

The first step to define a prior for the frequency coefficients of the quasi-static equivalent profile, is to transform into frequency domain all the available records of quasi-static test results in the area considered. If the number of quasi-static CPTu records available is M , M vectors of $q_{t-static}(u)$ are obtained. At different locations these coefficients $q_{t-static}(u)$ would differ due to soil heterogeneity, measurement characteristics and instrumental error.

In principle we assume a relatively wide area of provenance of the M quasi-static results, amongst which substantial heterogeneity is likely. This is expressed by means of a uniform prior distribution for each frequency component $q_{t-static}(u)$ in an interval bracketed by the minimum and maximum values obtained from the M transformed records. Alternative prior hypothesis for this variable are explored in the discussion section.

No distributions or statistics for strain-rate coefficient are available in the literature. Only average, maximum and minimum values of SRC have been reported. Given that lack of information we model strain-rate coefficient using a uniform distribution, simply defined by maximum and minimum values of SRC from literature (Table 1).

Very scarce information about model uncertainty for the tip cell method is available in the literature. Steiner et al. (2014) reported local estimates of σ_ε of about 40% of cone tip resistance at some depths. Actually, computing the mean value of standard error with the data reported by Steiner et al. (2014) it turns out to lie within $8-20\% \cdot \mu_{q_t}$, with μ_{q_t} mean value of quasi-static cone tip resistance. Based on this a uniform distribution within the interval $0 - 25\% \cdot \mu_{q_t}$ is adopted as prior for σ_ε .

4 Application example: dynamic CPTu offshore Nice airport

4.1 Geotechnical information

The case study concerns a landslide-prone area offshore Nice international airport (France). A large submarine landslide occurred in this area in 1979, causing significant material damage and claiming several lives. This has resulted in significant interest and during the last decades the

area has been intensively studied (e.g., Sultan et al. 2004; Dan et al. 2007; Leynaud & Sultan 2010; Steiner et al. 2015).

The geotechnical information considered for this study is reported in [Figure 4a](#). It corresponds to an area on the continental margin of about 1 x 1.5 km, located between 500 and 900 m offshore Nice airport and close to the shelf break. According to Sultan et al. (2010) the lithology all along the Nice margin is relatively uniform, mostly formed by detrital silty carbonates with some silty to fine quartz sand. As an example, a lithological description of three cores obtained by Sultan et al. (2004) is presented in [Figure 4b, c, d](#). It is clear that the lithology is dominated by fine grained sediments, with a very significant presence of clay. Laboratory analyses by Steiner et al. (2015) indicate a clay content between 20 and 30% for the clayey silt to silty clay (i.e., core 919-c [Figure 4b](#)). Liquid limits ω_L are up to 40% and the plasticity index IP lies between 10 and 25%.

Also reported in [Figure 4a](#) are the locations of nine 28 meter long quasi-static CPTu records obtained by Sultan et al. (2010). Measurements were obtained with the IFREMER Penfeld Penetrometer, which has a 10 cm² CPTu piezocone (Meunier et al. 2004). [Figure 5a](#) reproduces the first 5 m of those nine quasi-static q_t profiles.

The dynamic CPTu data analyzed were obtained using the MARUM FF-SW CPTu a dynamic penetrometer with a cone base section of 15 cm². Details regarding all mechanical and electronic components of this instrument are presented in Steiner et al. (2014), Stegmann et al. (2006). Distances between analyzed dynamic and quasi-static CPTu are reported in [Figure 5b, c](#).

In our study, the results of four dynamic CPTu are examined ([Figure 6](#)). Three of them (SW25a, b, c) were conducted at one location whereas SW23 is farther away. Tests SW25a and SW23 are characterized by relatively high impact velocities (about 9 m/s) and penetration depths up to 4-5 m ([Figure 6a, d](#)), (i.e., of about 250 observations). On the other hand, SW25b and SW25c are characterized by lower impact velocities (maximum of 1.2 m/s and 1.8 m/s, respectively) and penetration depths of about 2m ([Figure 6b, c](#)), (i.e., of about 90 observations).

4.2 SRC estimates through back-analysis of paired test

All the dynamic CPTu considered in this work were close to a quasi-static CPTu. Dynamic CPTu SW25a, b, c are paired with quasi-static CPTu 12s1 located at an approximate distance of about 24m. Dynamic CPTu SW23 is paired with quasi-static 11s6 located an approximate distance of about 23m.

The dynamic CPTu SW25a, b, c and SW23 were analyzed here with their paired quasi-static tests by applying the KS procedure and the three different *SRC* correction models described above. The *SRC* estimates thus obtained will be referred to as back-analyzed values. Results in terms of *SRC* and σ_ε are reported in Table 2. The value of σ_ε corresponds to the standard error between the converted dynamic profile and the paired quasi-static q_t profile.

Whatever the strain-rate law applied, higher *SRC* values characterized SW25a, c than SW25b and SW 23. The values obtained remained within the general ranges from literature (Table 1), except for the power law when applied to SW25c. The differences between SW25b and SW25c are noteworthy, as they correspond to closely located tests with similar impact dynamics, yet the back-analyzed *SRC* are not close. For the inverse hyperbolic sine law, the values obtained are close to the range 0.1-0.15 applied by Steiner et al. (2015). The standard error σ_ε from the back-analysis is very insensitive to the choice of strain-rate law, and it remained higher for SW25a than for the other tests – a fact that may be related to the presence of more heterogeneities in this profile.

4.3 Prior knowledge at Nice airport

The DCT frequency coefficients for all the nine quasi-static CPTu records in the area are presented in Figure 7. For each dynamic test analyzed the prior knowledge for the N frequency components of $q_{t-static}(u)$ was obtained from all the existing quasi-static test in the area, except for the paired test, which was excluded (12s1 for the SW25 and 11s6 for SW23, respectively). This means that the quasi-static data employed in the procedure was located at more than 300 m in average (and always more distant than 175 m) from SW23 and at around 1 km in average from the SW25.

A uniform prior knowledge is considered for *SRCs* in the interval bounded by the maximum and minimum values reported in Table 1. For the method error the prior is a uniform distribution within the domain $0 - 25\% \cdot \mu_{qt}$, with μ_{qt} the mean value of all the eight quasi-static unpaired CPTu records. A summary of the employed prior knowledge is given in Table 3.

4.4 Bayesian strain rate correction of dynamic CPTu

The outputs of the Bayesian updating procedure are probabilistic distributions for all the DCT coefficients of the equivalent quasi-static profile, for the *SRC* and for the transformation model precision σ_ε . These results can be exploited to obtain probabilistic estimates of a strain rate corrected quasi-static equivalent of the dynamic cone tip resistance. Unless otherwise stated, and

for reasons of space, we will present results only for the case of the logarithmic strain-rate correction model. A more exhaustive set of results may be found in Collico (2022).

Figure 8 presents, for the case of the dynamic CPTu SW25a, some key results of the TMCMC procedure. Figure 8a, reports the evolution of p_j coefficients indicative of a smooth transition from prior to posterior distribution (eq. 12). Figure 8b reports the distribution samples generated at the first stage, where $p_j = 0$, and samples are generated from the specified prior uniform distributions of SRC and σ_ε . Figure 8c presents the equivalent samples for $p_j = 1$, where the algorithm converges to the most plausible solution. The values of SRC and σ_ε obtained through back-analysis of a paired test are indicated with a red cross. It can be observed that, for this test, the samples at that final stage gather around the back-analyzed value.

Figure 8d reports the quasi-static cone tip profile acquired at the same location along with the dynamic one and the generated cone tip resistance profile at the last stage of TMCMC. The generated TMCMC profile is computed by applying the inverse discrete cosine function (eq. 10a) to the mean posterior estimates of the N frequency components of the DCT of $q_{t-static}(u)$. When compared with the measured paired quasi-static one, the generated TMCMC profile appears consistent on average but not in detail, (e.g., the local peak registered in both dynamic and static probes at 3.8 m depth is not present).

The results at the final stage obtained for SW25b, SW25c and SW23 as reported in Figure 9. It can be observed that the KS back-analyzed results lie within the scatterplot of equivalent samples, although the standard error obtained from the paired back analysis tends to lie close to the lower limit of the TMCMC estimates. Visual comparison of the generated CPTu profile from TMCMC, with the target paired CPTu record (Figure 9 suggest a better match at lower frequencies than at higher ones. It is worth noticing that equivalent samples for SW25b and SW25c profiles exhibits larger scatter (i.e., larger variance) with respect to SW25a and SW23 profiles. Such difference can be attributed to the lower number of dynamic observations that compose the corresponding dynamic CPTu profiles, resulting in a lower acceptance ratio and therefore larger variance of the joint posterior distribution.

The discrepancies between the quasi-static TMCMC profile and the quasi-static measurements are not surprising, as the TMCMC profile is not a strain rate corrected version of the dynamic profile. To obtain a strain-rate corrected version we should instead select a SRC from the posterior distribution and apply it to the dynamic measurement. Consideration of that distribution, as well

as that of the conversion error allow a probabilistic description of the dynamic to static CPTu transformation. The posterior mean of SRC (i.e., μ_{SRC}) and σ_ε (i.e., μ_{σ_ε}), computed as the mean of the generated last stage samples ($N_{samples} = 10000$ in this study), are unbiased estimates for the expected value of those parameters, conditioned on the data $E(\mu_{SRC}, \sigma_\varepsilon | \text{Data})$, (Ching and Wang 2016).

Posterior statistics (mean and standard deviation) for the SRC 's are reported in Table 4. The expected value of the posterior estimates of SRC for the logarithmic law is within 10% of the back-analyzed SRC , and the results are similar for the other cases. Table 4 also presents the statistics (mean and standard deviation) for the correction standard error. The mean values of σ_ε are generally very close to the value obtained from paired test back-analyses.

Posterior estimates of strain-rate coefficient and σ_ε may be employed to obtain credible intervals when dynamic CPTu are converted into quasi-static ones. This is illustrated Figure 10a, b, c, d reporting the converted cone tip resistance profiles obtained by applying the logarithm strain-rate correction. The average converted cone tip resistance profile (blue thick line) is computed with the expected value of the SRC from the generated equivalent samples. For reference, we also present a converted profile obtained using the average SRC value from literature (thick red line, see Table 1).

Bayesian 95% credible regions for the conversion (i.e., dark blue and light blue bands) are also reported in Figure 10. The narrow dark blue band reflects the uncertainty on the SRC estimate. It is obtained as the range of converted q_t profiles with SRC within the credible interval for this parameter ($\mu_{SRC} \pm 1.96 \sigma_{SRC}$). The wider light blue band reflects the uncertainty of SRC and that of the conversion, and is obtained by applying $\mu_{SRC} \pm 1.96$ updated standard error of SRC and mean estimate of σ_ε . The measured quasi-static result lies generally within the narrower credible region and almost always within the larger one.

5 Discussion

One attractive feature of Bayesian probabilistic models in geotechnical problems is their ability to incorporate informed engineering judgement (Vick 2002). The selection of prior for the quasi-static transformed profile is the aspect that, in this particular case, requires more judgement.

To obtain the results presented above we assumed a non-informative prior, leading to a uniform distribution for all frequency components. This gives equal weight to any observation in the area,

independently of how many times it is repeated. However, if the study area is characterized by relative uniform geotechnical and geological conditions it might be more appropriate to assume an informative prior, giving more credence to observed repetitions in the database. This can be implemented by using a normal distribution for the quasi-static prior.

We have reevaluated the case of the Nice airport using normal distributions as priors for the DCT components, with mean and variance obtained from the relevant set of quasi-static data in each case. Results in terms of expected value of quasi-static profile, equivalent sample scatter plot and converted profile are reported in [Figure 11a, b, c](#) and [Figure 12a, b, c](#) for SW25a and SW23, respectively. A posterior estimate of *SRC* and strain-rate model error σ_ε for each dynamic CPTu record is reported in [Table 5](#). By all these measures the results seem improved with respect to those obtained using the uninformative uniform prior. This is not very surprising because, as we noted above, the literature suggests that the Nice airport shelf is actually rather uniform.

In some cases, there might be fewer static CPTu profiles or the area might be more lithologically diverse than the selection of sites studied here. However, it is likely that in those cases the prior knowledge on the quasi-static profile will be very uninformative. To simulate this scenario, we have repeated the analysis for CPTu SW25a but now multiplying by a factor of three the interval width defining uniform knowledge for the DCT components. The results are illustrated in [Figure 13a, b](#).

The obtained q_t profile appears very rough and does not really approximate the actual paired quasi-static profile. The equivalent sample scatter plot for this simulation is reported in [Figure 13b](#). The scatterplot does not overlap the result from back-analysis. The poor performance of the algorithm is also evident in the high values of σ_ε and the low values of *SRC*, which are unusual for the local clay and silty clay lithology ([Figure 4c](#)). The process is then repeated for the remaining dynamic CPTu records (SW25b, SW5C, SW23). Posterior estimates of *SRC* and strain-rate model error σ_ε are reported in [Table 5](#), with similar results as those described previously.

Such example highlights how database heterogeneity seems an important factor in the TMCMC effectiveness. For the case study, horizontal and vertical heterogeneity within the proximal database was relatively small. The analyzed CPTu locations had lithologies composed mainly by fine clay sediments with medium plasticity (i.e., 60-80%) with interbedded layers of silt and fine sand. This corresponded to normally to slightly over consolidated sediments within the same geological setting (i.e., Var sedimentary system), all located within continental shelf French part of Ligurian margin (Steiner et al. 2015).

6 Conclusion

Using the proposed methodology, we have shown that it is possible to correct dynamic CPTu tests without the need for paired quasi-static tests. Using quasi-static data acquired at distances ranging from 300-1000 m from the converted test we attain almost the same precision in conversion that was attained with paired tests located at less than 25 m from the target. The computed quasi-static profiles are characterized by narrower uncertainty regions to those resulting from applying *SRC* minimum and maximum value from literature. These results are encouraging, as the method would facilitate the use of dynamic CPTu probes for offshore site investigation.

As in all Bayesian methods the role of the prior is very important. If the prior knowledge is very uninformative (wide variation of frequential component amplitudes), inconsistent results in terms of *SRC*, strain-rate model standard error and synthetic q_t profile are likely. This, however, is a situation that would correspond to very heterogenous sites, a feature that should be evident in the data and might be addressed by some zoning.

On the other hand, by applying a more informative knowledge (i.e., normal distribution) an improvement of accuracy prediction can be observed due to the generation of a more correlated synthetic q_t profile. Such prior knowledge seems more appropriate for study areas characterized by homogenous lithological features.

Although the method has been illustrated using conversion of cone tip resistance the procedure could be easily adapted to transform sleeve friction and/or pore pressure measurements from dynamic CPTu, using the relevant strain rate laws. Adaptation to other conversion models seems also straightforward, although it would require selection of model-specific random variables different from *SRC*.

Acknowledgment

This research received funding from the European Union's Horizon 2020 research and innovating programme under the Marie Skłodowska-Curie grant agreement No 721403.

Competing Interests Statement: The authors declare there are no competing interests.

Data Availability Statement: Data generated or analyzed during this study are available from the corresponding author upon reasonable request.

Notation

$q_{t-static}$ = corrected cone tip resistance acquired during quasi-static $CPTu$ test;

$q_{t-static}(u)$ = transformed corrected cone tip resistance within frequency domain u ;

$SRC_{log/exp/asinh}$ = strain-rate coefficient for logarithmic, exponential and inverse-sine hyperbolic strain-rate laws.

q_{t-dyn} = corrected cone tip resistance acquired during dynamic $CPTu$ test;

v_{dyn} = penetration velocity during dynamic $CPTu$ test

d_{dyn} = diameter of dynamic cone probe;

v_{ref} = constant reference velocity (2cm/s);

d_{ref} = diameter of quasi-static cone probe;

$h(\theta)$ = strain-rate model;

θ = vector of unknown random variables according to strain-rate model h ;

ξ = actual model response;

ε = strain-rate model error $N(\mu_\varepsilon, \sigma_\varepsilon)$;

μ_ε = mean value of model error;

σ_ε = standard error of strain-rate model;

N = number of data within $CPTu$ sounding record;

M = number of $CPTu$ soundings previously acquired;

References

- Augustesen, A., Liingaard, M., and Lade, P. V. 2004. Evaluation of time-dependent behavior of soils. *International Journal of Geomechanics*, 4(3), 137-156.
- Baecher, G. B., and Christian, J. T. (2005). *Reliability and statistics in geotechnical engineering*. John Wiley & Sons.
- Biscontin, Giovanna and Juan M. Pestana. 2001. "Influence of Peripheral Velocity on Vane Shear Strength of an Artificial Clay." *Geotechnical Testing Journal* 24(4):423–29.
- Bishop, C. M. (2006). "Pattern recognition and machine learning". *Information Science and Statistics* (Vol. 27). New York: Springer.
- Buhler, R. L., and Audibert, J. M. 2012. Rate-Effect Correction Methods for Free-Fall CPT Data In Deepwater Gulf of Mexico-An Operator's Perspective. In *Offshore Site Investigation and Geotechnics: Integrated Technologies-Present and Future*.
- Candès, Emmanuel J., Justin Romberg, and Terence Tao. 2006. "Robust Uncertainty Principles: Exact Signal Frequency Information." *IEEE Transactions on Information Theory* 52(2):489–509.
- Collico, S. 2022. Optimization of marine sediments characterization via statistical analysis, Doctoral dissertation, Universidad Politècnica de Catalunya, UPC.
- Collico, S., Arroyo, M., Urgeles, R., Gràcia, E., Devincenzi, M., and Pérez, N. 2020. Probabilistic mapping of earthquake-induced submarine landslide susceptibility in the South-West Iberian margin. *Marine Geology*, 429, 106-296.
- Ching, J., and Chen, Y. C. 2007. Transitional Markov chain Monte Carlo method for Bayesian model updating, model class selection, and model averaging. *Journal of engineering mechanics*, 133(7), 816-832.
- Ching, J. and Wang, J. S. 2016. "Application of the Transitional Markov Chain Monte Carlo Algorithm to Probabilistic Site Characterization." *Engineering Geology* 203:151–67.
- Chow, S H, C. D. O'Loughlin, D. J. White, and M. F. Randolph. 2017. "An Extended Interpretation of the Free-Fall Piezocone Test in Clay." *Geotechnique* 67(12):1090–1103.

Chung, S. F., M. F. Randolph, and J. A. Schneider. 2006. "Effect of Penetration Rate on Penetrometer Resistance in Clay." *Journal of Geotechnical and Geoenvironmental Engineering* 132(9):1188–96.

Contreras, L. F., Brown, E. T., and Ruest, M. 2018. Bayesian data analysis to quantify the uncertainty of intact rock strength. *Journal of Rock Mechanics and Geotechnical Engineering*, 10(1), 11–31. <https://doi.org/10.1016/j.jrmge.2017.07.008>

Dan, G., Sultan, N. and Savoye, B. 2007. "The 1979 Nice Harbour Catastrophe Revisited: Trigger Mechanism Inferred from Geotechnical Measurements and Numerical Modelling." *Marine Geology* 245(1–4):40–64.

Dayal, U. and Allen, J. H. 1975. "The Effect of Penetration Rate on the Strength of Remolded Clay and Sand Samples." *Canadian Geotechnical Journal* 12(3):336–48.

DeJong, J. T., R. A. Jaeger, R. W. Boulanger, M. F. Randolph, and D. A. J. Wahl. 2013. "Variable Penetration Rate Cone Testing for Characterization of Intermediate Soils." *Geotechnical and Geophysical Site Characterization 4 - Proceedings of the 4th International Conference on Site Characterization 4, ISC-4 1(April 2016):25–42.*

Gelman, A., Carlin, J. B., Stern, H. S., Dunson, D. B., Vehtari, A., and Rubin, D. B. 2013. *Bayesian*

data analysis. CRC press.

Ladd, C. C., Foot, R., Ishihara K., Poulos, H. G., and Schlosser F. 1977. "Stress-Deformation and Strength Characteristics." *Soil Mechanics and Foundation Engineering* 2, Tokyo. 421–94.

Lehane, B. M., C. D. O'loughlin, C. Gaudin, and M. F. Randolph. 2009. "Rate Effects on Penetrometer Resistance in Kaolin." *Geotechnique* 59(1):41–52.

Leynaud, D. and N. Sultan. 2010. "3-D Slope Stability Analysis: A Probability Approach Applied to the Nice Slope (SE France)." *Marine Geology* 269(March):89–106.

Meunier, J., Sultan, N., Jegou, P., and Harmegnies, F. 2004. First tests of penfeld: A new seabed penetrometer. *Proceedings of the International Offshore and Polar Engineering Conference*, 1, 338–345.

O'Loughlin, C. D., Richardson M. D., Randolph M. F., and Gaudin, C. 2013. "Penetration of Dynamically Installed Anchors in Clay." *Geotechnique* 63(11):909–19.

Oppenheim, A. V. and R. W. Schafer. 1999. DISCRETE-TIME SIGNAL PROCESSING. NJ: Upper Saddle River.

Randolph, M. F., Stanier, S. A., O'Loughlin, C. D., Chow, S. H., Bienen, B., Doherty, J. P., and Schneider, J. A. 2018. Penetrometer equipment and testing techniques for offshore design of foundations, anchors and pipelines. In Cone Penetration Testing 2018: Proceedings of the 4th International Symposium on Cone Penetration Testing (CPT'18), 21-22 June, 2018, Delft, The Netherlands (p. 3). CRC Press.

Randolph, M.F., and Hope, S. 2004 Effect of cone velocity on cone resistance and excess pore pressures. In Proceedings of IS Osaka - Engineering Practice and Performance of Soft Deposits, Osaka, Japan. Yodogawa Kogisha Co. Ltd. pp. 147–152.

Stegmann, S., Mörz, T., and Kopf, A. 2006. Initial Results of a new Free Fall-Cone Penetrometer (FF-CPT) for geotechnical in situ characterisation of soft marine sediments. Norwegian Journal of Geology 86(3).

Steiner, A., Kopf, A. J., L'Heureux, J. S., Kreiter, S., Stegmann, S., Hafliðason H., and Moerz, T. 2014. "In Situ Dynamic Piezocone Penetrometer Tests in Natural Clayey Soils - a Reappraisal of Strain-Rate Corrections." Canadian Geotechnical Journal 51(4):272–88.

Steiner, A., Kopf A. J., Henry, P., Stegmann S., Apprioual, R., and Pelleau, P. 2015. "Cone Penetration Testing to Assess Slope Stability in the 1979 Nice Landslide Area (Ligurian Margin, SE France)." Marine Geology 369(November):162–81.

Stoll, R. D., Sun Y. F., and Bitte I. 2007. "Seafloor Properties from Penetrometer Tests." IEEE Journal of Oceanic Engineering 32(1):57–63.

Sultan, N., P. Cochonat, M. Canals, A. Cattaneo, B. Dennielou, H. Hafliðason, J. S. Laberg, D. Long, J. Mienert, F. Trincardi, R. Urgeles, T. O. Vorren, and C. Wilson. 2004. "Triggering Mechanisms of Slope Instability Processes and Sediment Failures on Continental Margins: A Geotechnical Approach Triggering Mechanisms of Slope Instability Processes and Sediment Failures on Continental Margins: A Geotechnical Approach." (August 2018). doi: 10.1016/j.margeo.2004.10.011.

Sultan, N., Savoye, B., Jouet, G., Leynaud, D., Cochonat, P., Henry, P., Stegmann, S., and Kopf, A., J. 2010. "Investigation of a Possible Submarine Landslide at the Var Delta Front (Nice Continental Slope, Southeast France)." Canadian Geotechnical Journal 47(4):486–96.

Vick, S. G. 2002. Degrees of belief: Subjective probability and engineering judgment. ASCE Publications.

Wang, Y., Au, S. K. and Cao, Z. 2010. "Bayesian Approach for Probabilistic Characterization of Sand Friction Angles." *Engineering Geology* 114(3–4):354–63.

Zhang, J., Zhang, L., and Tang, W. H. 2009. "Bayesian Framework for Characterizing Geotechnical Model Uncertainty." *Journal of Geotechnical and Geoenvironmental Engineering* 135(7):932–40.

Zhao, T., Hu, Y., and Wang, Y. 2018. "Statistical Interpretation of Spatially Varying 2D Geo-Data from Sparse Measurements Using Bayesian Compressive Sampling." *Engineering Geology* 246:162–75.

Zhao, T., Xu L., and Wang, Y. 2020. "Fast Non-Parametric Simulation of 2D Multi-Layer Cone Penetration Test (CPT) Data without Pre-Stratification Using Markov Chain Monte Carlo Simulation." *Engineering Geology* 273(January):105670.

Zhou, W. H., Tan, F., and Yuen, K. V. 2018. Model updating and uncertainty analysis for creep behavior of soft soil. *Computers and Geotechnics*, 100, 135-143.

Tables

Table 1. Literature strain-rate coefficients values for cone tip correction in fine-grained sediments

Formulation	Logarithmic			Inv Sin. hyp			Power law		
Sources	(Dayal & Allen, 1975; Randolph & Hope 2004; Steiner et al., 2014)			(Steiner et al., 2014)			(Steiner et al., 2014; Chow et al., 2007)		
	Lower	Average	Upper	Lower	Average	Upper	Lower	Average	Upper
SRC_{qt}	0.1	0.15	0.25	0.043	0.076	0.11	0.03	0.05	0.08

Table 2. Back-analyzed SRC and σ_ε values.

ID paired quasi-static CPT _u	ID dynamic CPT _u	Unknown variables	Log law	Power Law	Inv – hyp sin law
CPT _u 12s1	SW25a	μSRC_{qt}	0.23	0.08	0.085
		σ_ε [kPa]	47	46	46
	SW25b	μSRC_{qt}	0.14	0.065	0.061
		σ_ε [kPa]	20	20	21
	SW25c	μSRC_{qt}	0.2	0.084	0.069
		σ_ε [kPa]	26	28	26
CPT _u 11s6	SW23	μSRC_{qt}	0.145	0.064	0.062
		σ_ε [kPa]	30	30	30

Table 3. Prior knowledge of unknown random variables.

	Unknown random variable	minimum μ	maximum μ	Density distribution
$q_{t-static}$	$q_{t-static}(u)$	–	–	uniform
SRC	SRC_{log}	0.1	0.25	uniform
	SRC_{exp}	0.03	0.09	uniform
	SRC_{asinh}	0.043	0.1	uniform
Model uncertainty	σ_ε	0.1	25% μ_{qt}	uniform

Table 4. Posterior knowledge of strain-rate coefficients and model error σ_ε .

ID CPTu	Unknown variables	log – law			power – law			inv. Sin – hyp. – law		
		back – analyzed μ	Post. μ	Post. σ	back – analyzed μ	Post. μ	Post. σ	back – analyzed μ	Post. μ	Post. σ
SW 25a	$SRCq_t$	0.23	0.227	0.01	0.08	0.087	0.003	0.085	0.09	0.0054
	σ_ε	47	46	1.15	46	46.7	1.46	46	46.65	0.87
SW 25b	$SRCq_t$	0.14	0.145	0.03	0.065	0.054	0.006	0.061	0.06	0.004
	σ_ε	20	22.57	0.3	20	27.3	3.8	21	23.6	1.5
SW 25c	$SRCq_t$	0.2	0.22	0.034	0.084	0.071	0.008	0.069	0.075	0.011
	σ_ε	26	32	3.95	28	27.9	4.85	26	24.24	1.4
SW 23	$SRCq_t$	0.145	0.136	0.02	0.064	0.061	0.0045	0.062	0.07	0.006
	σ_ε	30	43	2.98	30	28	0.8	30	35	2.33

Table 5. Posterior knowledge of strain-rate coefficients and model error σ_ε by applying a wider uninformative prior knowledge.

log – law								
ID CPTu	Unknown variables	back analyzed	Uninformative		Wider Uninformative		Informative	
		μ	Post. μ	Post. σ	Post. μ	Post. σ	Post. μ	Post. σ
SW 25a	$SRCq_t$	0.23	0.227	0.01	0.05	0.0017	0.24	0.009
	σ_ε	47	46	1.15	96	1.06	44.3	2.48
SW 25b	$SRCq_t$	0.14	0.145	0.03	0.066	0.012	0.137	0.02
	σ_ε	20	22.57	0.3	64.3	1.41	31.3	3.3
SW 25c	$SRCq_t$	0.2	0.22	0.034	0.061	0.008	0.19	0.028
	σ_ε	26	32	3.95	63	1.74	33.52	3.65
SW 23	$SRCq_t$	0.145	0.136	0.02	0.06	0.03	0.135	0.015
	σ_ε	30	43	2.98	97.3	1.41	34	4.8

Figures captions

Figure 1. Example of back-calculation for logarithmic stain-rate law. The red line is the CDF for converted $q_t - dynamic$ for different SRC_{log} values, while the black line is the CDF of $q_t - static$.

Figure 2. Flowchart of proposed methodology.

Figure 3a) $q_t - static(z)$ profile. b) Corresponding $q_t - static(u)$ amplitude by applying eq. (10b).

Figure 4. a) Location of retrieved core samples and quasi-static CPTu as reported by Sultan et al. (2004) and dynamic CPTu considered for strain-rate correction. b) Visual core description of core 919-gc collected at the shelf break off the Nice international airport (southeastern France) according to Steiner et al. (2015). b) gravity core lithology of GoeB13946. c) gravity core lithology of GoeB13926.

Figure 5. First 5 m of quasi-static CPTu profiles offshore Nice airport from Sultan et al. (2004).

Figure 6. Corrected cone tip resistance q_t and penetration velocity profiles for: (a) SW 25a test; (b) SW 25b; (c) SW 25c; and (d) SW 23

Figure 7. Quasi-static prior information in Nice: amplitude of DCT coefficients for all the CPTu

Figure 8. a) p_j coefficient values at different j-th stage. b) Equivalent samples generated at stage $p_j=0$. c) Equivalent samples generated at stage $p_j=1$. d) q_t profile generated from TMCMC at stage $p_j=1$.

Figure 9. Equivalent samples of SRC and σ_ε at final TMCMC stage ($p_j=1$) and dynamic and quasi-static measured profiles alongside the profile generated from TMCMC at stage $p_j=1$ for: a) Test SW 25b, b) Test SW 25c, c) Test SW 23.

Figure 10. Converted dynamic cone tip resistance for logarithmic strain-rate law a) SW 25a. b) SW 25b. c) SW 25c d) SW23.

Figure 11. Bayesian analysis results for SW 25a when the quasi-static prior is Gaussian. a) Generated q_t profile from TMCMC. b) Equivalent samples scatter plot at final stage c) measured and converted profiles, including credible intervals.

Figure 12. Bayesian analysis results for SW23 when the quasi-static prior is Gaussian. a) Generated q_t profile from TMCMC. b) Equivalent samples scatter plot at final stage c) measured and converted profiles, including credible intervals.

Figure 13. Bayesian analysis results for SW 25 a when the quasi-static prior is a wide uniform distribution. a) Generated q_t profile from TMCMC. b) Equivalent samples scatter plot at final stage c) measured and converted profiles, including credible intervals.

Figures

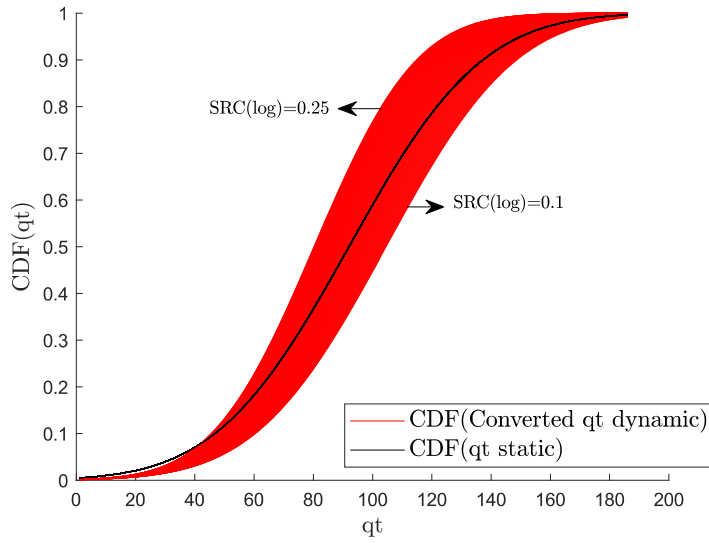


Fig. 1

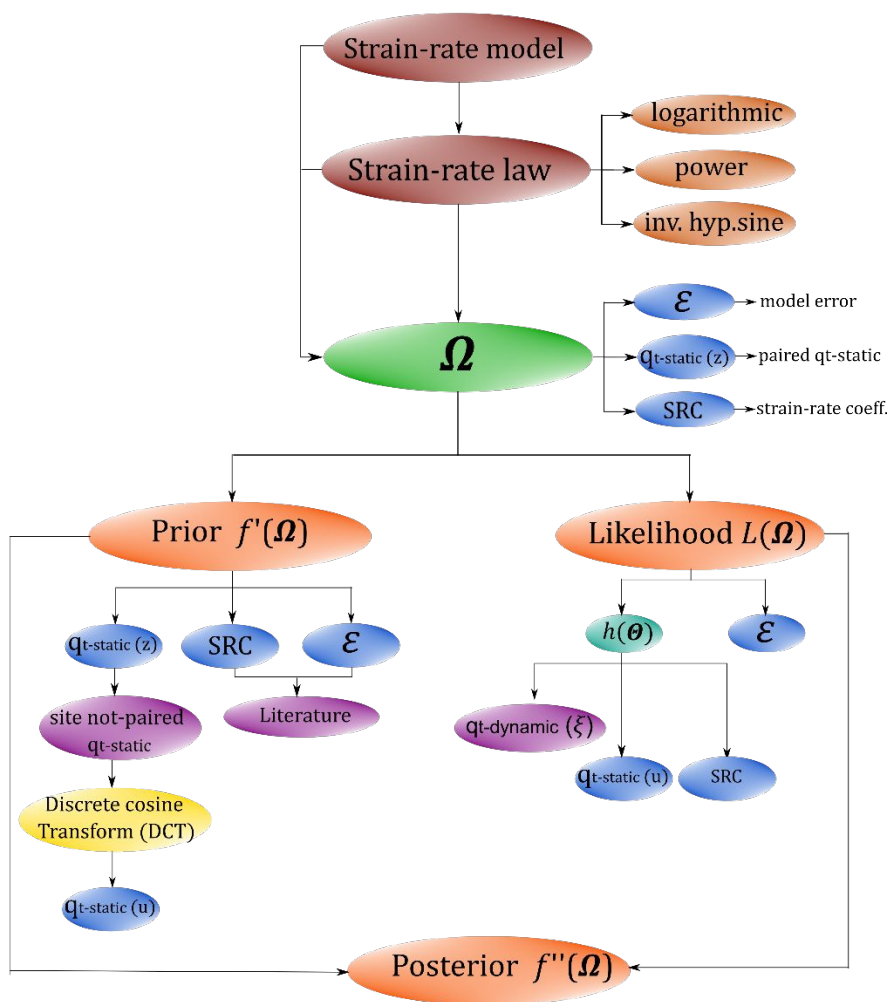


Fig. 2

Can. Geotech. J. Downloaded from cdnsiencepub.com by UNIV POLITECNICA DE CATALUNYA on 11/20/22
For personal use only. This Just-IN manuscript is the accepted manuscript prior to copy editing and page composition. It may differ from the final official version of record.

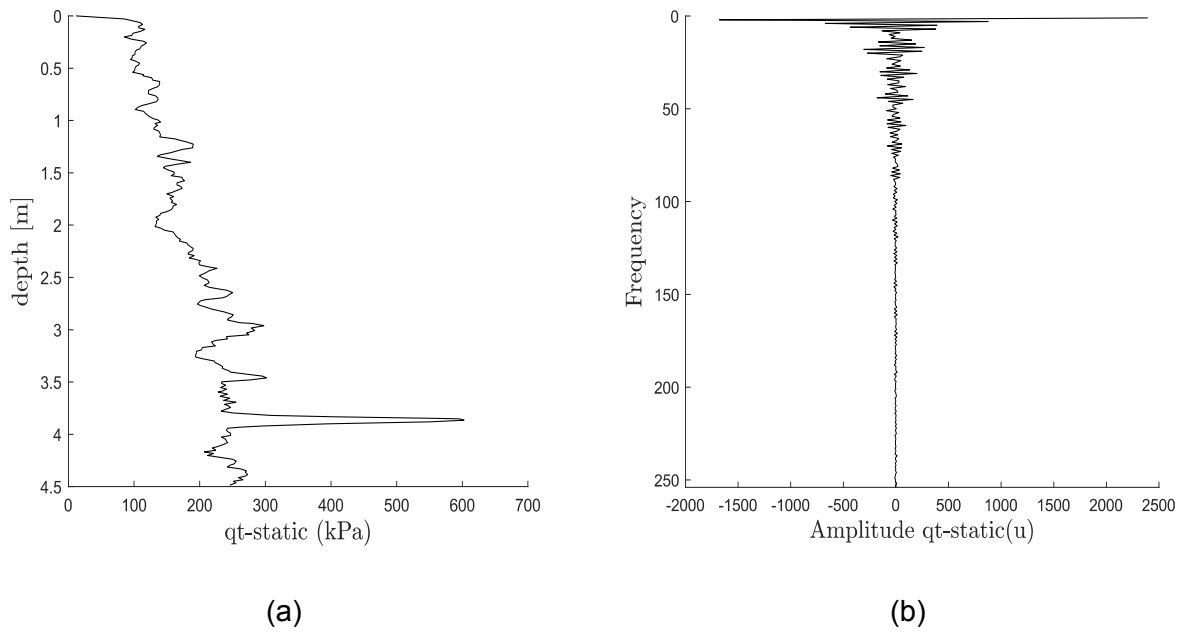


Fig. 3

Can. Geotech. J. Downloaded from cdnservicepub.com by UNIV POLITECNICA DE CATALUNYA on 11/20/22
For personal use only. This Just-IN manuscript is the accepted manuscript prior to copy editing and page composition. It may differ from the final official version of record.

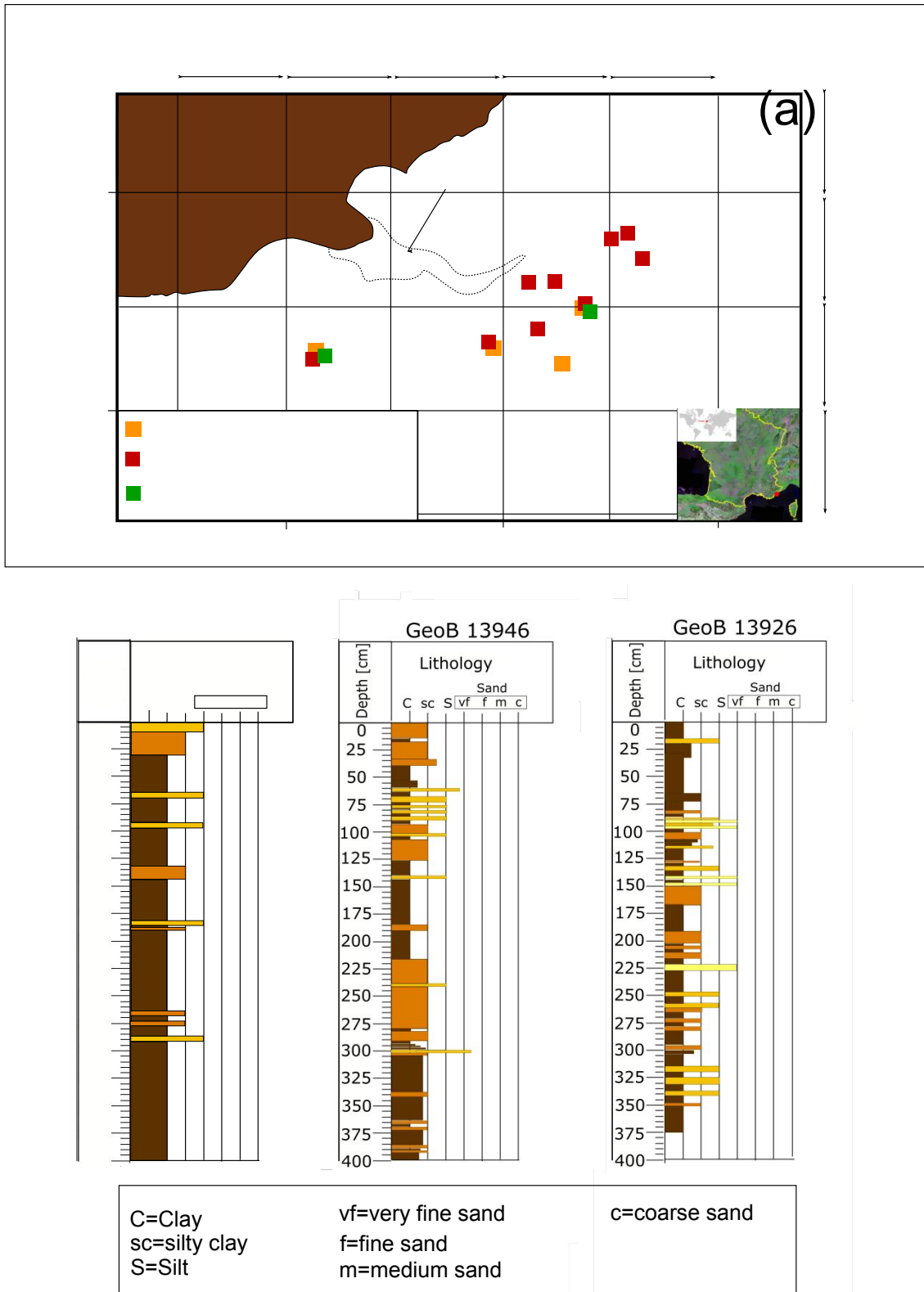


Fig. 4

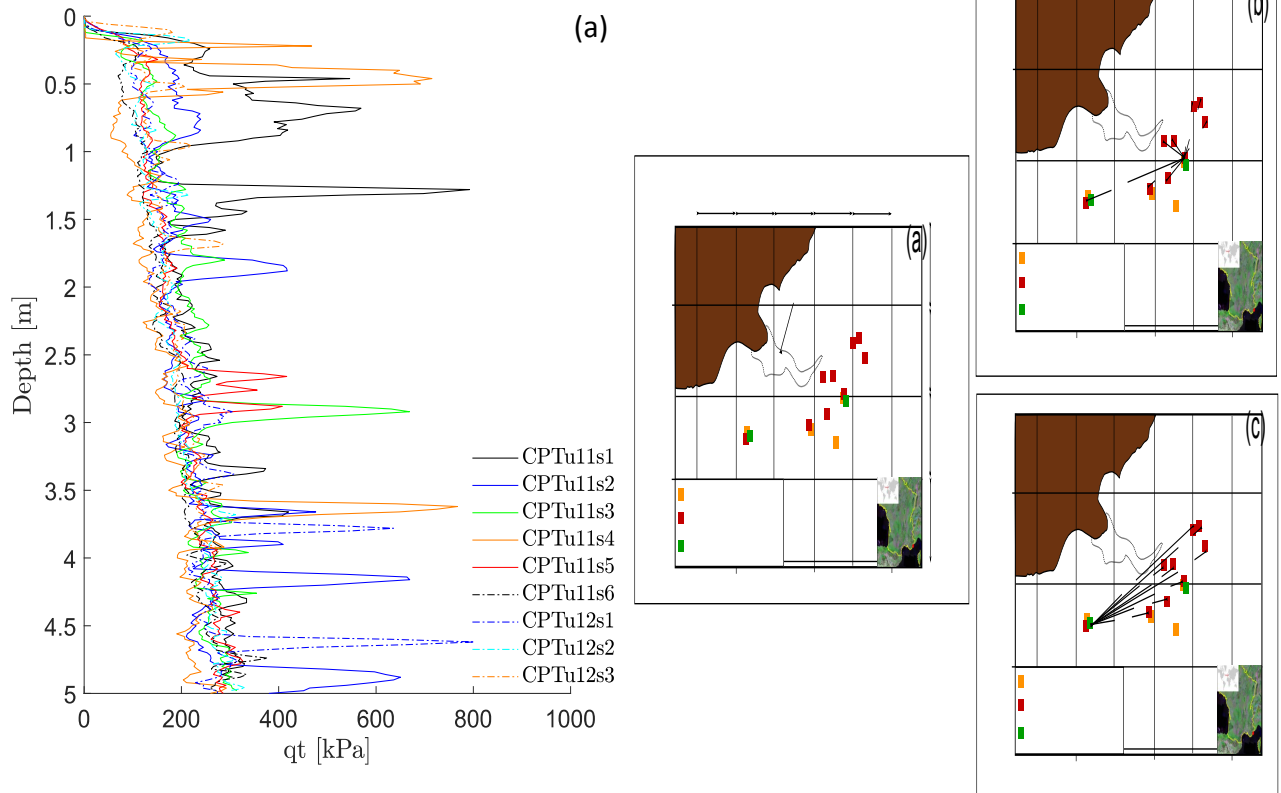


Fig. 5

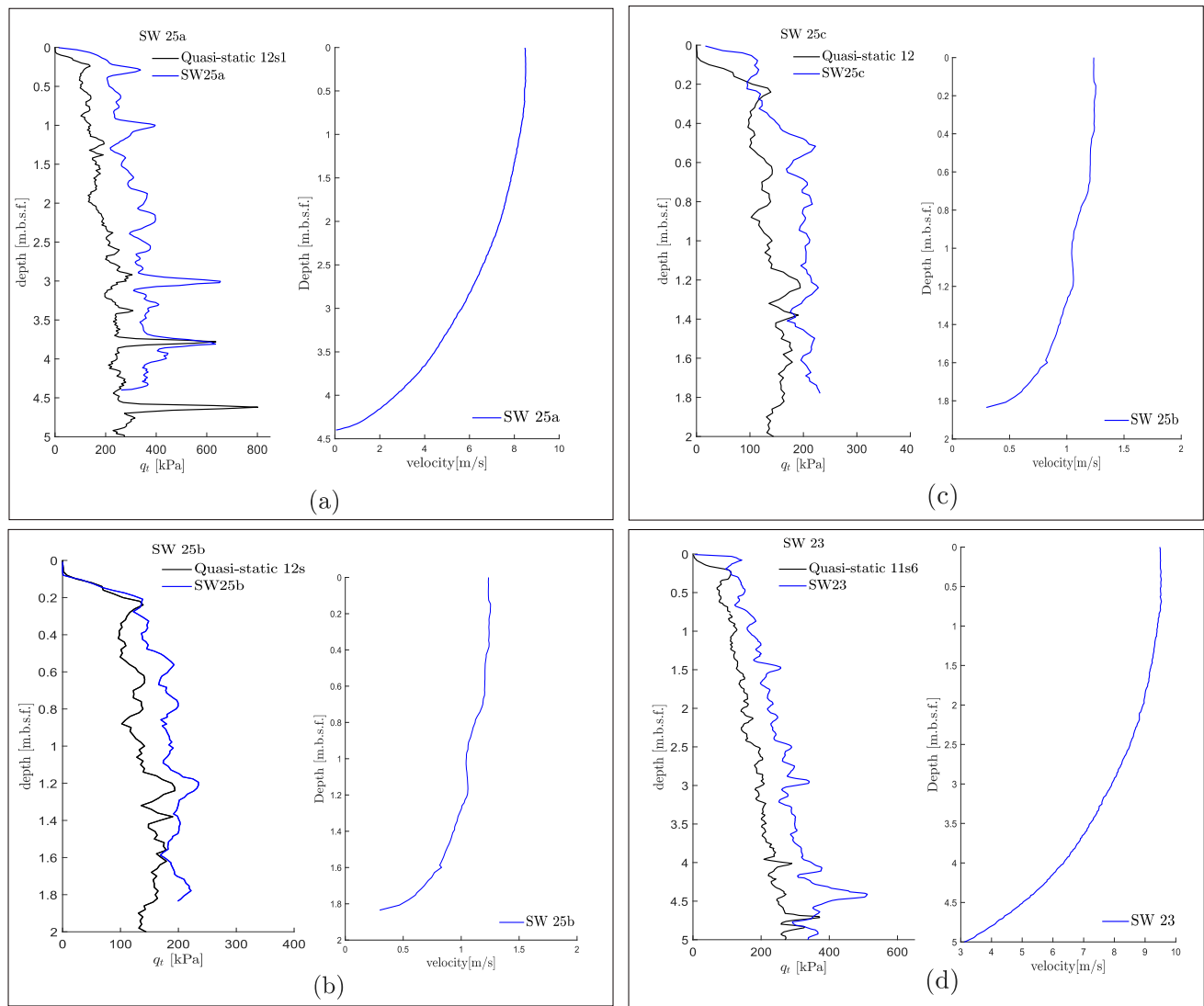


Fig. 6

Can. Geotech. J. Downloaded from cdsciencepub.com by UNIV POLITECNICA DE CATALUNYA on 11/20/22
For personal use only. This Just-IN manuscript is the accepted manuscript prior to copy editing and page composition. It may differ from the final official version of record.

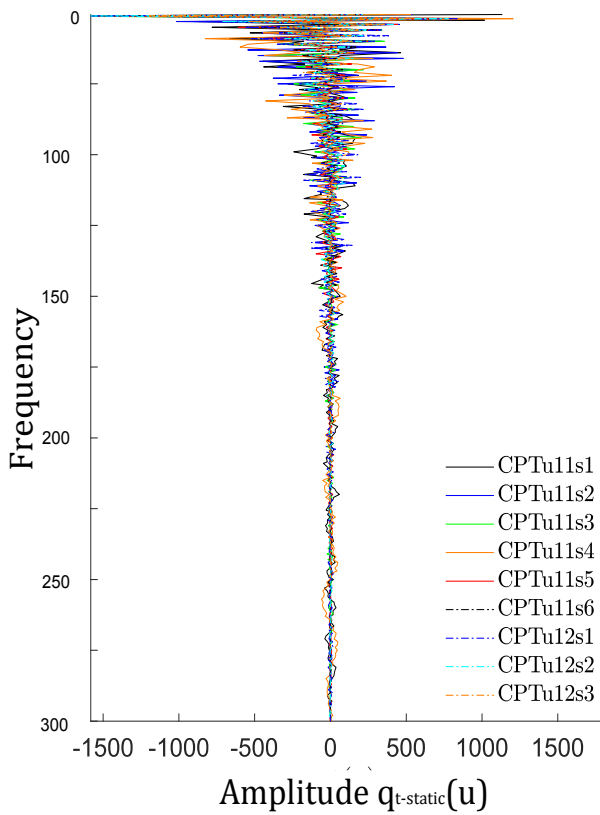
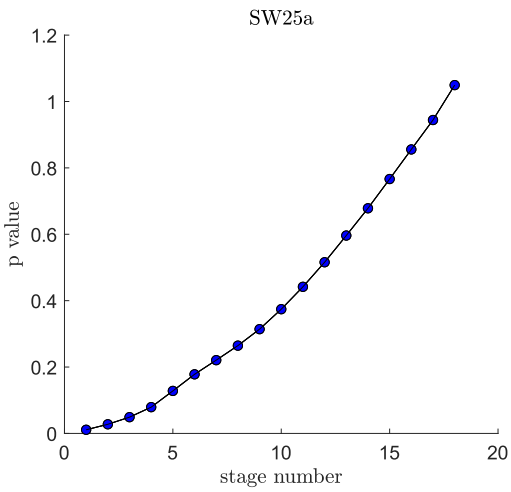
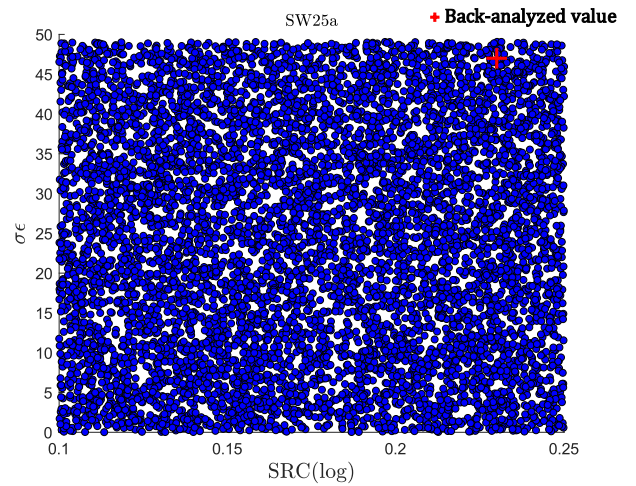


Fig. 7



(a)



(b)

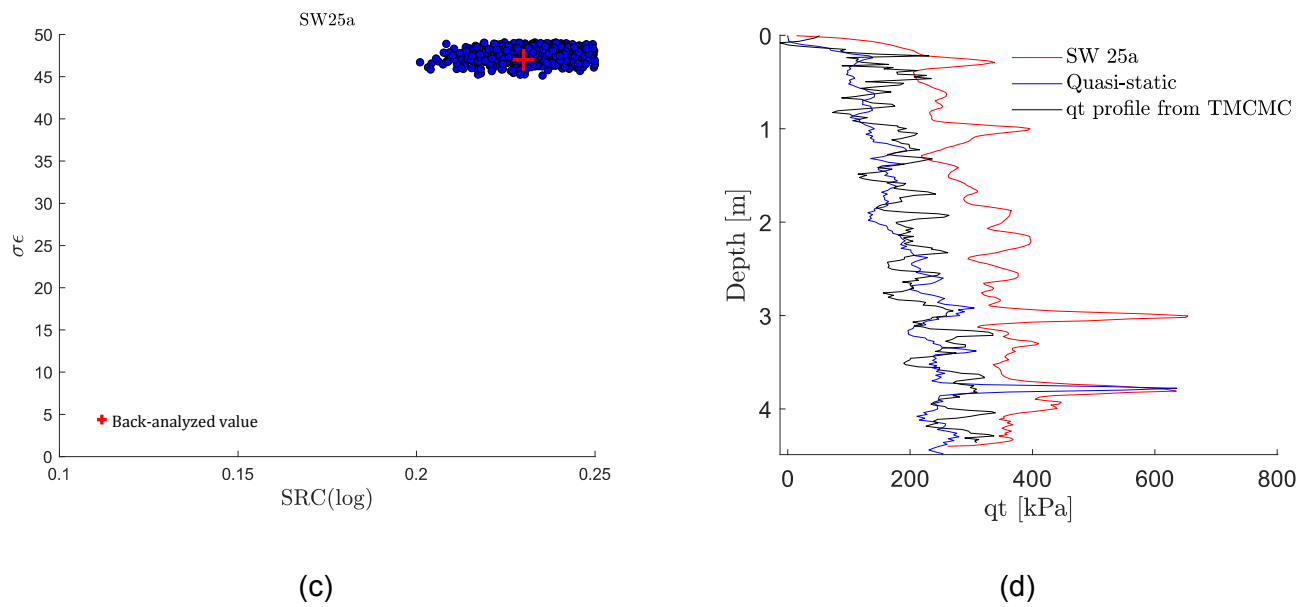


Fig. 8

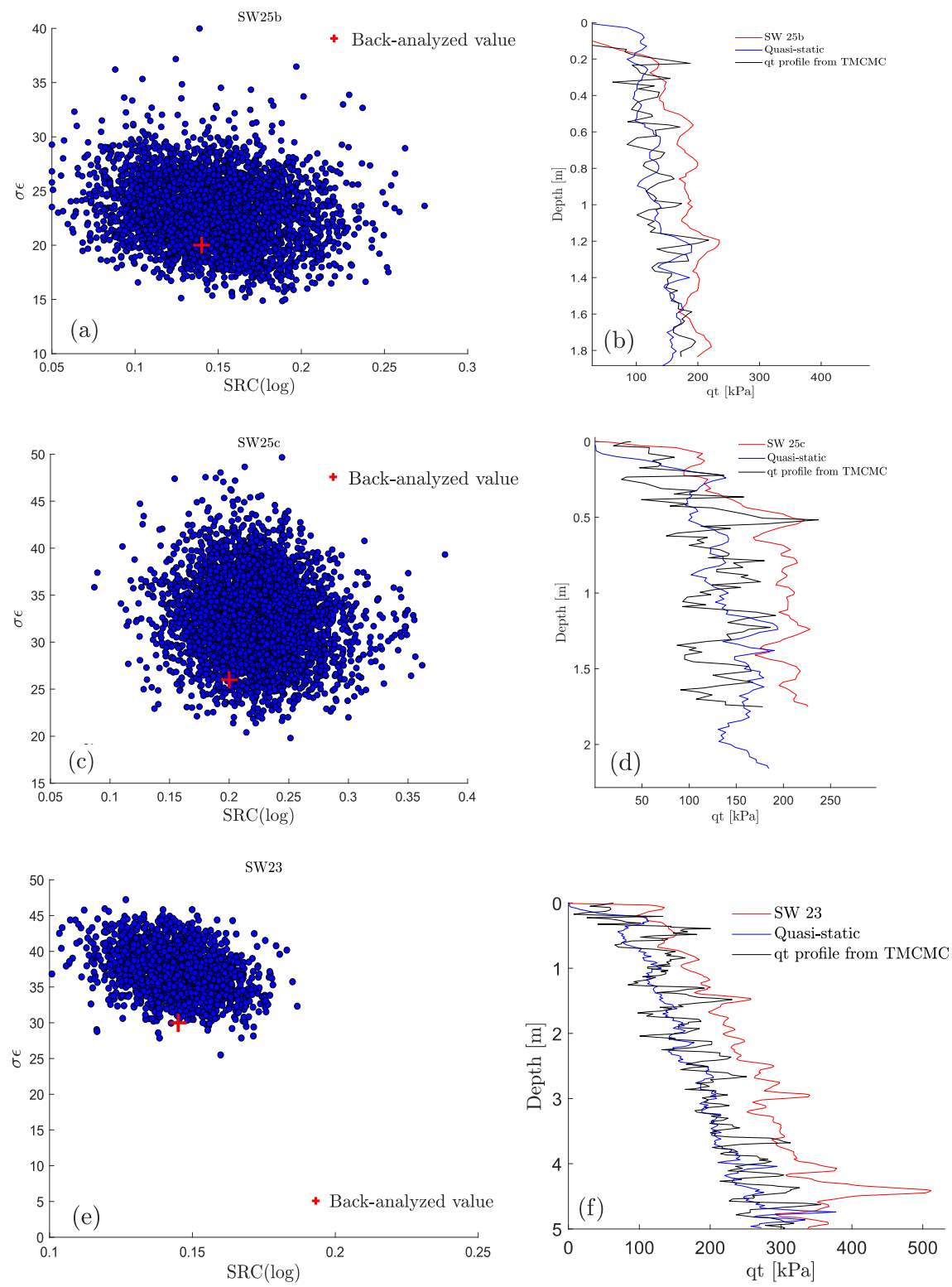


Fig. 9

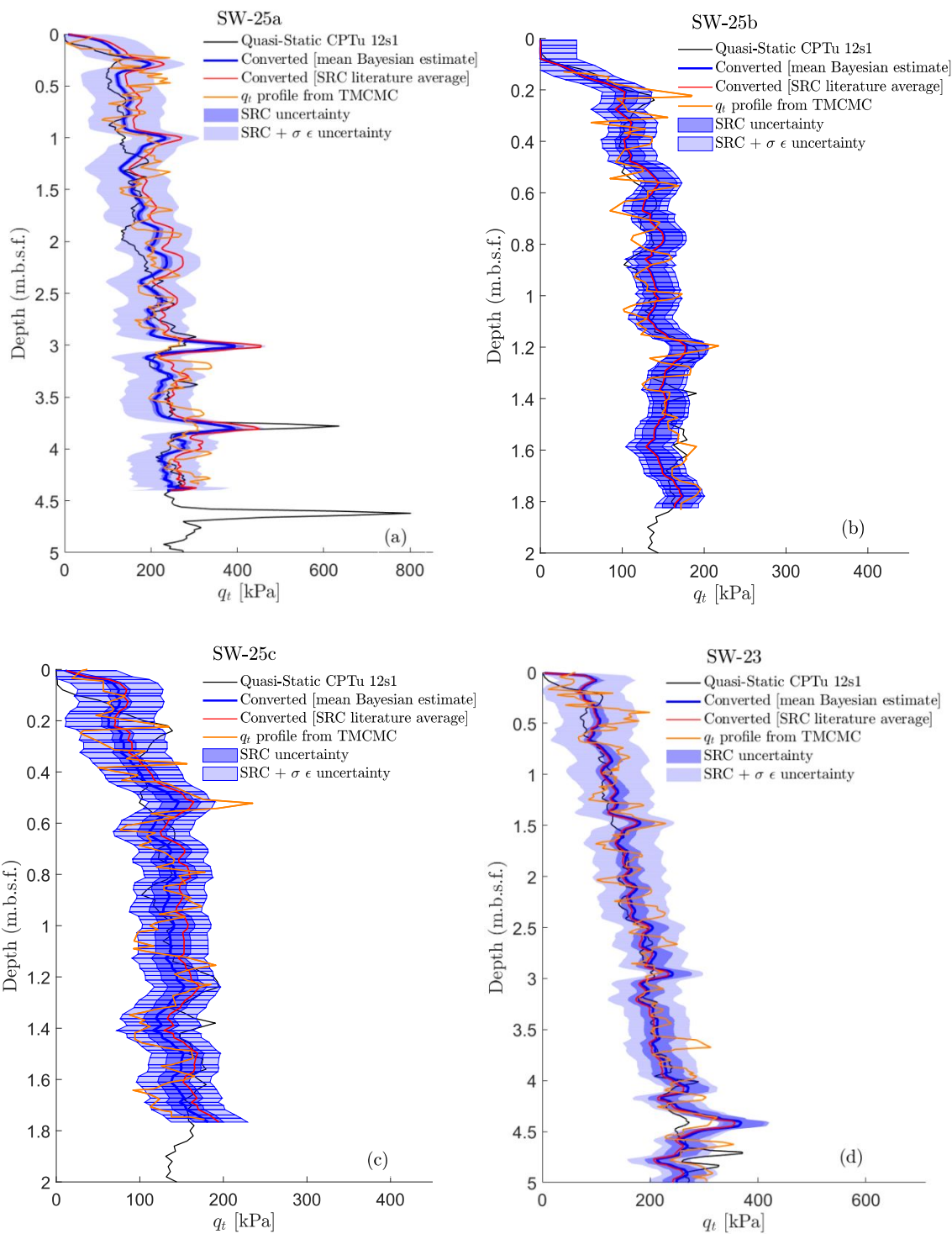
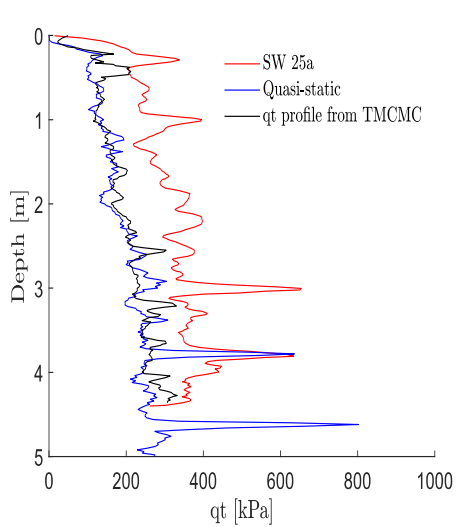
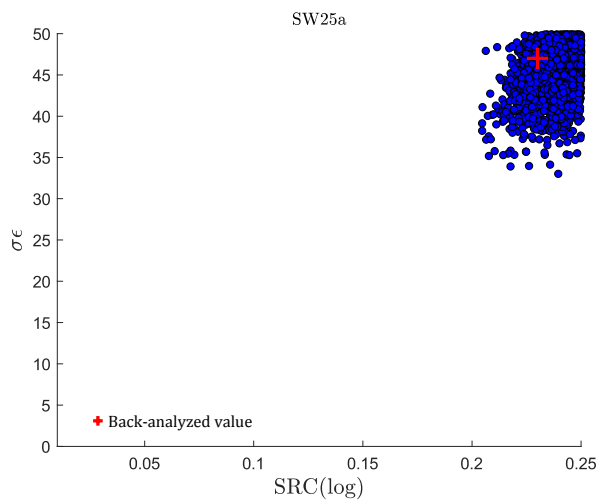


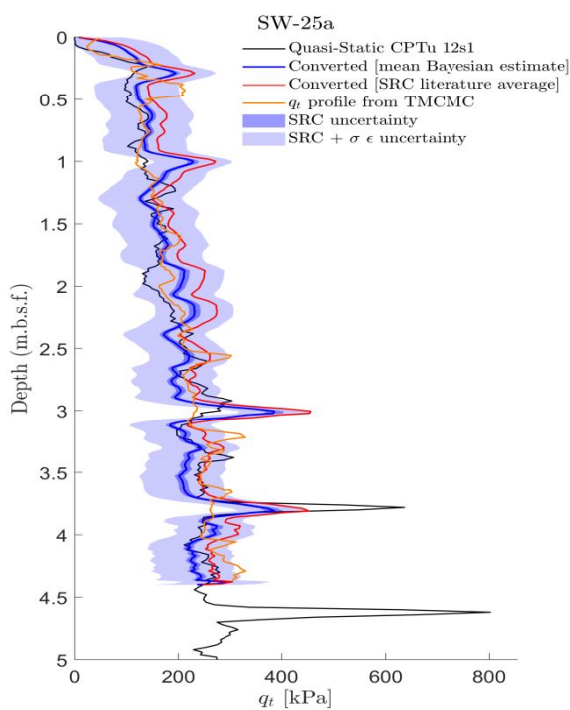
Fig. 10



(a)



(b)



(c)

Fig. 11

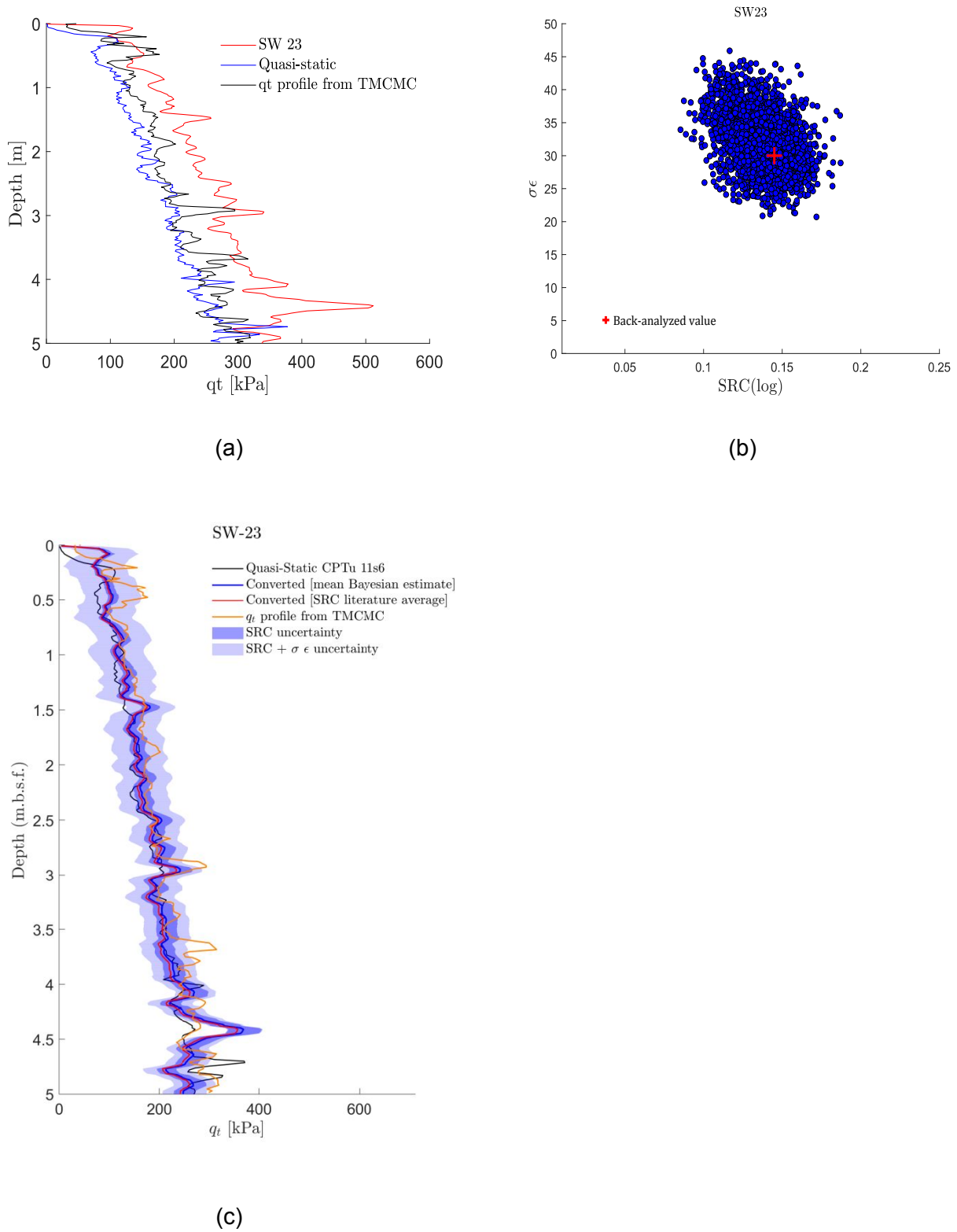
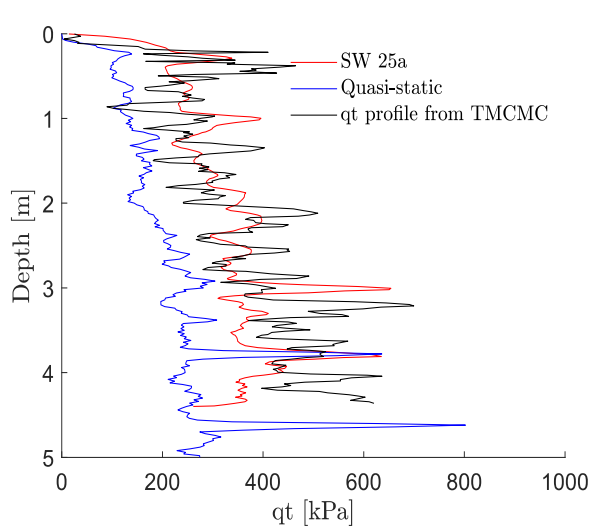
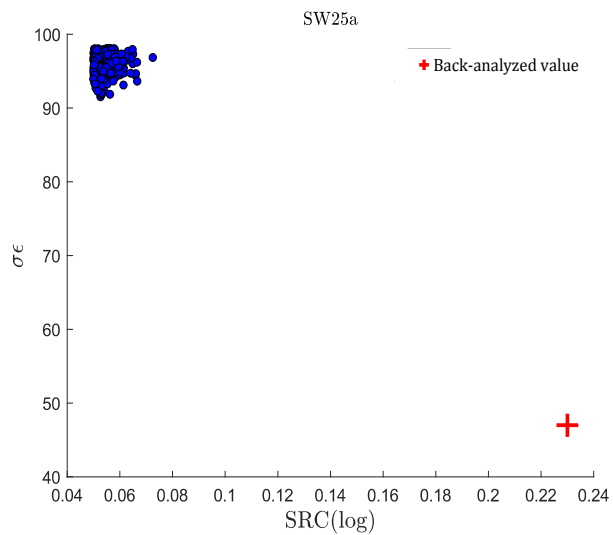


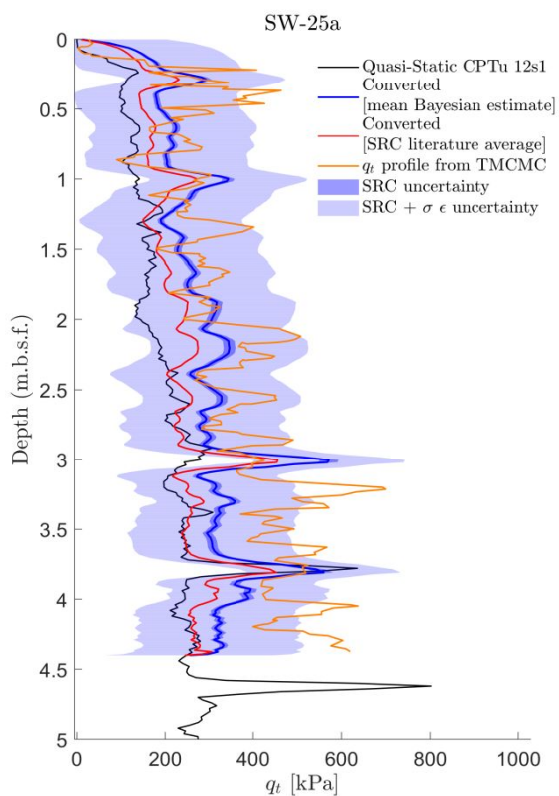
Fig. 12



(a)



(b)



(c)

Fig. 13